POLITECNICO
MILANO 1863

SCUOLA DI INGEGNERIA INDUSTRIALE
E DELL'INFORMAZIONE

EXECUTIVE SUMMARY OF THE THESIS

Characterization of PAGAT polymeric gel for Hadron Therapy dosimetry

TESI MAGISTRALE IN NUCLEAR ENGINEERING – INGEGNERIA NUCLEARE

AUTHOR: RICCARDO BRAMBILLA

ADVISOR: PROF. MARIO MARIANI

ACADEMIC YEAR: 2022-2023

1. Introduction

Radiotherapy is one of the most effective techniques for the treatment of cancers, its general principle consisting in delivering high radiation doses to the tumoral tissue to destroy or inactivate cells following DNA damage. With the advent of conformal radiotherapy, for which the dose distribution is conformed to the tumor target through collimators or exploiting the physical properties of the radiation beam, dosimetry has become even more important in the process of quality assurance (QA) and treatment plan verification. Since conventional dosimetric devices are not able to directly measure tridimensional dose distributions due to their 1D or 2D nature and often suffer from a poor tissue equivalence, the interest in chemical gel dosimetry has surged and throughout many studies promising results have been observed in conventional radiotherapy with photons and electrons (IMRT, IORT) [1].

This thesis work focused on the characterization and study of the PAGAT gel for its use in Hadron Therapy (HT) dosimetry. The PAGAT gel dosimeter, investigated for the first time by Venning *et al.* in 2004 [2], is a normoxic polyacrylamide and gelatin dosimeter (PAG) employing tetrakis hydroxymethyl phosphonium chloride (THPC) as an anti-oxidant. Compared to other gel dosimeters, these polymeric gels do not have the diffusion limitations of Fricke-type gels and the oxygen inhibition issue of anoxic polymeric formulations is avoided using THPC as anti-oxidant.

PAGAT gel response was studied after irradiation with high linear energy transfer (LET) particle beams employed in HT. This kind of radiotherapy makes use of accelerated hadrons for the treatment of surgically inoperable or radioresistant tumors and due to their physical and radiobiological properties, a more conformal dose deposition is achieved compared to conventional types of radiotherapy, better sparing healthy tissues located around the tumor. Up to now, few studies have been reported regarding the use of gel dosimeters with high-LET particles. In these studies, good agreements have been observed in terms of geometrical information, while a strong suppression in dose response at depths near the Bragg peak was measured due to a decrease in sensitivity [3], [4]. The aim of the thesis work was

to verify literature results irradiating PAGAT gel with proton and carbon ion beams at different irradiating conditions. The dosimeter analysis was performed using spectrophotometric and Magnetic Resonance Imaging (MRI) measurements.

2. Materials and methods

The PAGAT gel composition and its preparation was obtained from the literature. Acrylamide (AAm) and N,N′-methylene-bis-acrylamide (Bis) are the monomers, mono-vinyl and divinyl respectively, whose polymerization is induced by the interaction with the radiation. While AAm forms long, linear chains with no crosslinking, Bis is capable of forming several types of links (knots, loops, doublets) and is used as a crosslinking agent to increase the rigidity of the polymeric structure. As stated before, THPC acts as an anti-oxidant, scavenging 0_2 molecules which, due to their high radical affinity, would inhibit the polymerization mechanism. To improve the scavenging ability of THPC, it is important that deionized water is employed as a solvent during preparation. As suggested by previous studies, an additional concentration of p-nitrophenol was incorporated as inhibitor to reduce the sensitivity of the dosimeter in order to extend the linearity range and compensate high-dose saturation of the dose response [5]. Lastly, the role of gelatin as a gelling agent is mainly to provide a three-dimensional matrix through which the polymers cannot diffuse, thus stabilizing the response of the dosimeter. Table 1 summarizes the composition of the gels prepared in this thesis work.

Table 1. PAGAT gel composition. The % refers to weight percentage.

Species	Quantity
AAm	3%
Bis	3%
Gelatin	5%
Deionized water	89%
p-nitrophenol	2.5 ppm
THPC	10 mM

2.1. Gel preparation

During the preparation process, AAm and Bis are dissolved in 55% of deionized water volume while heating and stirring until the monomer and cross-linker are completely dissolved. Meanwhile, porcine skin gelatin is added in the remaining 45% of water volume and, after both solutions are clear, they are allowed to cool down before being mixed together to prevent heat-induced polymerization. The proper amount of p-nitrophenol and THPC are then added drop-wise while stirring to ensure their uniform distribution. The resulting dosimetric solution is eventually poured into different containers based on their intended use.

Samples for calibration and stability assessment consisted in 5 mL PMMA spectro-photometric cuvettes. Phantoms for volumetric dose mapping were prepared in 0.5 L HDPE hollow cylinders with screw tops. After preparation, the samples were stored in a refrigerator at around 7 °C to allow the gelatin to solidify. Irradiation was performed after at least 12 hours to ensure the stabilization of the dosimetric composition. Refrigeration was maintained at all times possible to prevent gelatin liquefaction.

2.2. Irradiation

The gel dosimeters were irradiated with monoenergetic proton and carbon ion beams generated by the synchrotron accelerator at the Centro Nazionale di Adroterapia Oncologica (CNAO) facility in Pavia, Italy. The synchrotron extraction energy ranges from 60 MeV for protons up to a maximum of 400 MeV/u (4800 MeV) for carbon ions. All irradiations were performed using the vertical beamline of the second treatment room at CNAO where a precise robotic patient positioning system allowed consistent delivery positions between successive irradiations.

The cuvettes were horizontally positioned in groups of four, and the beam was spread out laterally using an active paint modality, covering a 7.2 x 7.2 cm area. To ensure tissue equivalence and mitigate the buildup effects, a support structure consisting of water-equivalent RW3 plastic slabs was used acting as a frame for the samples. The beam energies were carefully selected to keep the samples at the depth-dose profile plateau to minimize dose gradients in the longitudinal direction and allow the groups of four samples to

be irradiated uniformly. The irradiation scheme included doses of 1 Gy, 2 Gy, and 4 Gy using monoenergetic protons with extraction energy of 97.54 MeV (corresponding to a Bragg peak at 70 mm depth in water) and 174.87 MeV (201 mm), as well as monoenergetic carbon ions of 181.17 MeV/u (70 mm).

For acquiring the volumetric response, the phantoms were positioned vertically and irradiated from the bottom using single-spot beams at various energies. Three phantoms were irradiated: two using monoenergetic protons at energies corresponding to 70 mm (97.54 MeV) and 101 mm (118.20 MeV), and one using a monoenergetic carbon ion beam at 90 mm (208.58 MeV/u) energy.

2.3. Dosimeter analysis

The gel dosimeter analysis involved optical and MRI readouts conducted at different time intervals after irradiation to evaluate the dose response stability. UV-Vis spectrophotometry and MRI scanning were used for cuvette analysis, while MRI was exclusively used for volumetric phantoms. Initial measurements were performed at least two days after irradiation to allow the polymerization response to develop.

Optical analysis of the cuvettes utilized a LAMBDA 650 UV/Vis spectrophotometer (Perkin Elmer), with a sampling wavelength of 550 nm and a scanning time of 0.2 s. The goal of the analysis was to construct dose-absorbance curves, characterizing the polymerization response in terms of sensitivity and linearity range. To achieve this, the mean absorbance of blank specimens was subtracted from that of irradiated samples, and a linear interpolation with dose values was performed. Temporal stability was assessed by repeating measurements over a two-month period post-irradiation.

Magnetic resonance analysis was conducted using a clinical MRI scanner at the CNAO facility, a 3 T Magnetom Skyra Fit (Siemens). While the cuvettes were characterized using both MRI and optical techniques, volumetric phantoms were scanned using only MRI analysis to capture their three-dimensional dose information. A multi-slice multi-echo pulse sequence was used for all dosimeters involving 32 echo times (TE) ranging from 20 to 640 ms, with 20 ms increments. The voxel dimensions measured 1.4 x 1.4 x 1.4 mm. The MRI raw data comprised T2-weighted images capturing signal intensity at different echo times and an image reconstruction algorithm in the Matlab environment was adapted to generate R2 maps. The algorithm involved several steps aiming at fitting the decaying signal intensity pixel-by-pixel using maximum-likelihood estimation with χ^2 minimization and constructing R2 maps of the scanned objects.

2.4. Data analysis

The statistical analysis and the fitting of the data were aimed at calculating dosimetric parameters and quantifying gel performance.

For the analysis of the characterization samples the following quantities have been considered: *sensitivity*, defined as the slope of the linear curve fitting the dose values against the instrument response; *dose resolution*, expressing the minimal detectable dose difference with a given level of confidence and whose value is proportional to the standard deviation in dose of the irradiated sample; *precision*, which describes the relative dispersion between independent measurement results of the dosimeters irradiated at the same dose; *accuracy*, which evaluates the relative difference between the measured dose compared to the prescribed one.

The analysis performed on the volumetric phantoms was intended to evaluate the three-dimensional abilities of the gel by comparing depth-dose curves and transversal distributions with reference profiles taken with well-established methods.

3. Results and discussion

3.1. Characterization

The purpose of this phase was to verify a linear dose response and determine dosimetric parameters under different irradiation conditions. Spectrophotometric cuvettes were exposed to protons and carbon ions to investigate any dependence on LET. The energy dependence was also explored by irradiating with protons at two different energies. The dosimetric performance was evaluated using both spectrophotometric and MRI measurements and the temporal evolution of signal was assessed by conducting optical analysis

at five different times during a period of more than two months after irradiation.

A good linearity of the dose response was confirmed using optical measurements for all inspected doses. The dosimetric quantities derived from the optical analysis showed dose resolutions below 1 Gy and a mean accuracy of around 1-2%. The sensitivity values were comparable to previous studies, but the mean precision was higher (of the order of 10%), potentially due to uncertainties in the fabrication process. A slight decrease in sensitivity was observed as the proton energy and LET increases.

The temporal stability of the optical response was evaluated by considering the evolution of the sensitivity for the 70 mm proton irradiation samples. The stability analysis of PAGAT dosimeters demonstrated similar results to those irradiated with photons or electrons, suggesting that the particle type does not significantly affect it.

MRI measurements also confirmed a good linearity for the entire dose range. However, the sensitivity for the samples irradiated with 70 mm protons was considerably different, possibly indicating an energy or LET dependence, although it is probable that noise due to low MRI resolution might have contributed to the difference. This affected the dose resolution as values higher than 1 Gy were observed. Mean accuracy values were also higher compared to optical measurements but remained below 7%, while mean precision values ranged between 10% and 20%.

In Figure 1, the optical response of the characterization samples irradiated with protons and carbon ions is given.

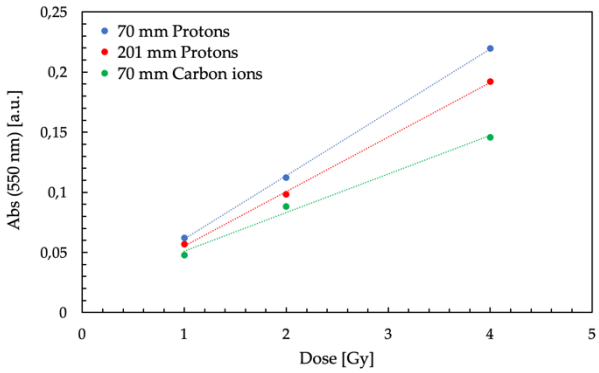

Figure 1. Optical response comparison of the characterization tests. Linear fitting curves are shown through the dotted lines. Uncertainties range from 0.002 to 0.02.

3.2. Volumetric response

The analysis on cylindrical phantoms aimed at assessing the volumetric response of PAGAT gels in terms of dose profiles along the irradiation direction and transversal dose distributions. Three phantoms were irradiated with single-spot beams: two with protons at 70 mm and 101 mm, and one with carbon ions at 90 mm.

MRI scanning was conducted at least 6 days after irradiation to allow the polymeric response to develop. The MRI readout involved a multiple spin echo sequence, and the T2-weighted images were processed to obtain R2 maps. The depth-dose profiles were extracted from the R2 maps by selecting pixels in the axial region of the cylinder and averaging their R2 values. These curves were compared with reference profiles measured using ionization chambers in water, with the peaks normalized to 1 for easier quantification of the quenching effect.

For the 70 mm proton irradiation, the depth-dose profile showed good agreement with the reference profile in the plateau and the first part of the Bragg peak, with a slight underestimation at the beginning of the plateau. An underestimation of approximately 35% at the Bragg peak confirmed the presence of quenching due to increased LET in the distal part of the peak. The geometrical position of the peak in was well recorded compared to the reference curve.

The 101 mm proton irradiation exhibited good agreement with the reference profile in the plateau region up to approximately 60 mm depth. The quenching effect was more pronounced, with an underestimation of around 55% at the Bragg peak suggesting that the LET dependence of the dosimeter sensitivity could be affected by the extraction energy of the particles.

The 90 mm carbon ion irradiation profile showed similar characteristics to the proton profiles, with slight underestimation in the plateau region and increasing quenching as the LET increased at higher depths. The underestimation at the Bragg peak was around 60%, the largest among the three cases. The dose tail in the distal part of the ion depth-dose curve, caused by projectile fragmentation, was well recorded.

The overall results confirmed previous literature findings, showing under-response of the PAGAT gel at the Bragg peak region where the LET increases. The magnitude of underestimation

appeared to be energy-dependent, with higher quenching observed for the 101 mm proton irradiation compared to the 70 mm proton irradiation. The gel response at the Bragg peak for the 90 mm carbon ion profile showed the largest underestimation due to the higher LET and hence lower gel sensitivity. Good agreement was observed between the gel and reference curves in the plateau region and at the fragmentation tail for carbon ions, indicating that the gel dose response is not significantly altered for low-LET values. The ability of the PAGAT dosimeter to accurately capture the geometrical information, such as the position of the Bragg peaks, could be valuable for non-absolute dosimetry in profile verification for highly conformal HT treatments. Figure 2 reports the depth-dose curve resulting from the 101 mm proton irradiation compared to the reference profile.

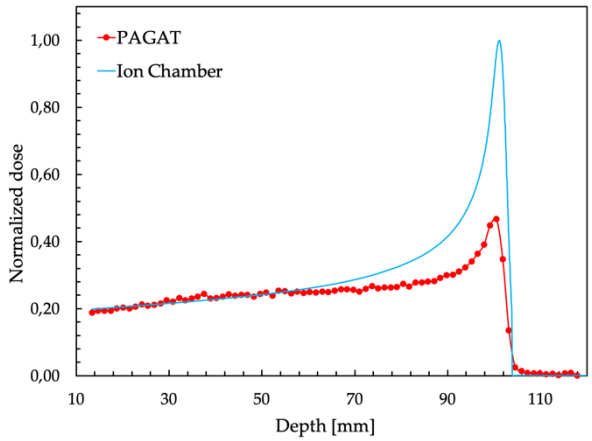

Figure 2. Normalized depth-dose profile for 101 mm (118.20 MeV) proton single-spot beam. The two curves were normalized at a depth of 50 mm.

In addition to the depth-dose profiles, the transversal dose distributions perpendicular to the beam direction were investigated. The R2 maps obtained from MRI were sampled along directions perpendicular to the cylinder axis and the resulting distributions were compared to experimental profiles recorded by radiochromic films. The irradiation of these films is performed in air, that is with no interface medium between the beam and the film, and for this reason the transversal dose profiles of the gels were taken along planes located at the bottom of the cylinders from which the beams entered the phantoms. The gel system performed well in recording the geometrical information, with very good agreement between the curves. The differences were mainly observed in the 90 mm carbon ion distribution, where the full width at half maximum (FWHM) recorded by the gel was approximately 10% larger than that obtained by the radiochromic film. However, this difference could be attributed to noise contributions in the MRI images, which became more significant for the smaller width of the carbon ion dose profile, and also to the finite spatial resolution of the MRI analysis, which, in this case, is of the same order of magnitude of the profile FWHM. The transversal profiles did not show any under-response due to the quenching effect, confirming that the gel dose response was not altered for low-LET values in the initial part of the depth-dose profile. The result of analysis for the 70 mm proton irradiation is shown in Figure 3.

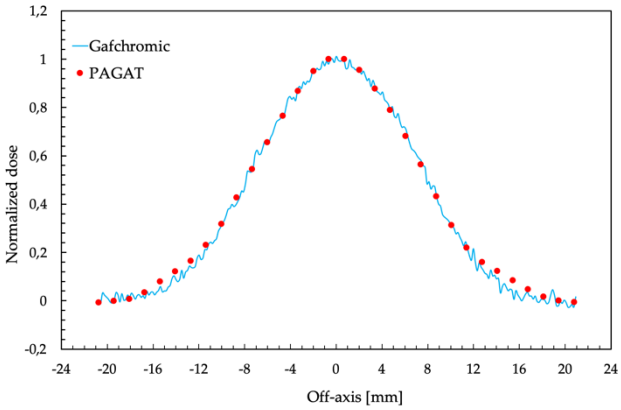

Figure 3. Transversal dose distribution for 70 mm proton single-spot beam. The two curves were normalized to their value at 0 mm off-axis. The gel profile was sampled at approximately 15 mm depth from the bottom of the phantom.

4. Conclusions

Polymeric gel systems offer high potential for the verification of dose profiles in Bragg-peak dominated hadronic irradiations due to their three-dimensional nature and excellent spatial resolution. The good temporal stability due to lack of diffusion-related signal degradation makes PAGAT a reliable recording medium for months after irradiation.

During the characterization phase using cuvette samples, spectrophotometric and MRI measurements showed good linearity up to 4 Gy. Optical analysis revealed slight energy and LET dependencies, while MRI measurements highlighted the need for pulse sequence optimization to improve signal-to-noise ratio (SNR) and eventually dose resolution.

Volumetric dose mapping conducted on cylindrical phantoms yielded excellent results for geometrical profile verification as the dimensions of the recorded dose deposition were in very good agreement with the reference profiles. However, high-LET quenching in the Bragg peak region caused an underestimation of the normalized dose. Carbon ion irradiation exhibited the highest under-response, with a 60% shortfall compared to the reference profile, while lower energy proton irradiation had a 35% underestimation at the peak. Future developments in PAGAT dosimeters for HT should address the issue of high-LET quenching. Possible strategies include constructing LET calibration curves to correct the under-response at the Bragg peak or exploring new gel compositions with reduced LET dependence. Standardized and optimized MRI sequences should be defined to fully exploit the 3D spatial resolution of gel dosimeters by reducing imaging artifacts and improving SNR.

5. Bibliography

[1] C. Baldock *et al.*, "Polymer gel dosimetry," *Phys Med Biol*, vol. 55, no. 5, 2010, doi: 10.1088/0031-9155/55/5/R01.

[2] A. J. Venning, S. Brindha, B. Hill, and C. Baldock, "Preliminary study of a normoxic PAG gel dosimeter with tetrakis (hydroxymethyl) phosphonium chloride as an anti-oxidant," *J Phys Conf Ser*, vol. 3, pp. 155–158, Jan. 2004, doi: 10.1088/1742-6596/3/1/016.

[3] M. Hillbrand *et al.*, "Gel dosimetry for three dimensional proton range measurements in anthropomorphic geometries," *Z Med Phys*, vol. 29, no. 2, pp. 162–172, May 2019, doi: 10.1016/j.zemedi.2018.08.002.

[4] H. Gustavsson, S. Å. J. Bäck, J. Medin, E. Grusell, and L. E. Olsson, "Linear energy transfer dependence of a normoxic polymer gel dosimeter investigated using proton beam absorbed dose measurements," *Phys Med Biol*, vol. 49, no. 17, pp. 3847–3855, Sep. 2004, doi: 10.1088/0031-9155/49/17/002.

[5] G. Magugliani *et al.*, "Practical role of polymerization inhibitors in polymer gel dosimeters," in *Nuovo Cimento della Societa Italiana di Fisica C*, Italian Physical Society, Nov. 2020. doi: 10.1393/ncc/i2020-20147-7.